

Longitudinal Development of Extensive Air Showers: Hybrid Code SENECA and Full Monte Carlo

Jeferson A. Ortiz,* Gustavo Medina-Tanco, and V. de Souza
Instituto de Astronomia, Geofísica e Ciências Atmosféricas
Universidade de São Paulo,
Caixa Postal 9638, São Paulo, SP 01065-970, Brasil

New experiments, exploring the ultra-high energy tail of the cosmic ray spectrum with unprecedented detail, are exerting a severe pressure on extensive air shower modeling. Detailed fast codes are in need in order to extract and understand the richness of information now available. Some hybrid simulation codes have been proposed recently to this effect (e.g., the combination of the traditional Monte Carlo scheme and system of cascade equations or pre-simulated air showers). In this context, we explore the potential of SENECA, an efficient hybrid tridimensional simulation code, as a valid practical alternative to full Monte Carlo simulations of extensive air showers generated by ultra-high energy cosmic rays. We extensively compare hybrid method with the traditional, but time consuming, full Monte Carlo code CORSIKA which is the de facto standard in the field. The hybrid scheme of the SENECA code is based on the simulation of each particle with the traditional Monte Carlo method at two steps of the shower development: the first step predicts the large fluctuations in the very first particle interactions at high energies while the second step provides a well detailed lateral distribution simulation of the final stages of the air shower. Both Monte Carlo simulation steps are connected by a cascade equation system which reproduces correctly the hadronic and electromagnetic longitudinal profile. We study the influence of this approach on the main longitudinal characteristics of proton-induced air showers and compare the predictions of the well known CORSIKA code using the QGSJET hadronic interaction model.

PACS numbers: 96.40.Pq, 96.40.-z, 13.85.-t

I. INTRODUCTION

Since the very first observations, ultra-high energy cosmic rays (UHECR) have been an open question and a priority in astroparticle physics. Their origin, nature and possible acceleration mechanisms are still a mystery. In the last decades many experiments such as Volcano Ranch [1, 2], Haverah Park [3], Yakutsk [4], Fly's Eye [5, 6], HiRes [7] and AGASA [8, 9] have contributed for the study of UHECR's, setting up the existence of such high energy particles. Shortly, the Pierre Auger Observatory will begin to explore them in unprecedented detail [10, 11].

Due to the very low flux of high energy cosmic rays, measuring extensive air showers (EAS) is the only possible technique to learn about the shape of the UHECR spectrum and their chemical composition. Two different ways have been historically applied to observe and analyze EAS's: ground array of detectors and optical detectors. Surface detectors measure a lateral density sample and trigger in coincidence when charged particles pass through them. Optical detectors (i.e., fluorescence detectors) observe the longitudinal profile evolution by measuring the fluorescence light from atmospheric nitrogen excitation produced by the ionization of the secondary charged particles (essentially electrons and

positrons). The combination of shower observables (such as lateral density, the depth of maximum shower development (X_{\max}) and number of muons (N_{μ}) at detector observation level) and simulation techniques is the current way to obtain information about the primary energy, composition and arrival direction. For this purpose the shower simulation should provide all possible, and ideally the necessary, information to interpret measurements of shower parameters. We suggest the reference [12] which is an interesting summary of experimental results from highest energy cosmic ray measurements, focused on data and analyzes that became available after 1999.

Many modern shower simulation packages have been developed over the years. Most of them are based on the Monte Carlo method and simulate complete high energy showers with well described fluctuations in the first particle interactions and realistic distributions of energy of shower particles. Unfortunately, the calculation of the gigantic showers induced by cosmic rays with energies above 10^{18} eV becomes a very difficult technical problem. This is due to the huge number of created secondary particles that have to be followed in the Monte Carlo method. As a consequence the direct simulation of the shower following each individual particle becomes practically impossible and the computation time takes too long.

Recently, different ways of calculating the air shower development have been proposed [13, 14]. Most of them combine the traditional Monte Carlo scheme with a system of electromagnetic and hadronic cascade equations.

*Electronic address: jortiz@astro.iag.usp.br

In a new one dimensional approach [15] pre-simulated pion-induced showers are described with parametrizations and then are superimposed to pion and kaon particles after their first interaction points are simulated by the Monte Carlo method.

In the present work we analyze extensively the results obtained by the SENECA [16] code. The SENECA simulation approach is based on the Monte Carlo calculation of the first and final stages of the air shower development, and on a cascade equation system that connects both stages reproducing the longitudinal shower development. We explore mainly the fast air shower generation for different primary energies. As an application of this approach we investigate the main longitudinal shower characteristics of proton, iron nucleus and gamma initiated air showers up to ultra-high energy, as predicted by the QGSJET [17, 18] hadronic interaction model. We compare SENECA results with the well tested CORSIKA (COsmic Ray Simulations for KAscade) simulation code [19].

This paper is structured as follows. In Sec. II we briefly describe the hybrid approach and the air shower modelling. In Sec. III the method is applied to study the longitudinal development and the shower observables as well. Our main intention is to compare our predictions to calculations performed with the CORSIKA shower generator, in order to verify the stability of the hybrid code and the reliability of the its results, in the sense of being useful to several experimental applications. We have made several calculations for gamma, iron nucleus and proton initiated showers with different energy thresholds, using the thinning procedure for the Monte Carlo simulation scheme. Average and fluctuation values of X_{\max} and S_{\max} , their correlations and distributions are presented. The number of electrons (N_e) and muons (N_μ) have been analyzed at different observation levels. Also, we show a comparison between CORSIKA and SENECA CPU time requirements for proton showers at different primary energies. Section IV summarizes our results.

II. SENECA APPROACH AND THE AIR SHOWER MODELLING

The main goal of this approach is the generation of EAS's in a fast manner, obtaining the correct description of the fluctuations in showers and giving the average values for the shower characteristics. The detailed technical information about the SENECA package can be obtained in [16, 20]. Even though the SENECA code describes both longitudinal and lateral air shower developments, the simulation scheme is used here to generate large statistics of longitudinal shower profiles applicable mainly to the present fluorescence detectors, such as Pierre Auger Observatory [21] and HiRes [7, 22], as well to the future telescope EUSO [23].

For the present work we track explicitly every particle with energy above the fraction $f=E_0/1.000$, where E_0 is

the primary shower energy, studying in detail the initial part of the shower. All secondary particles with energy below the mentioned fraction are taken as initial conditions to initialize a system of hadronic and electromagnetic cascade equations (see the suggested references). We use the cascade equations up to several minimum electromagnetic energy thresholds of 1, 3.16, 10, 31.6 and 100 GeV for the electromagnetic component (E_{\min}^{em}) and $E_{\min}^{\text{had}}=10^4$ GeV for the hadronic component. Hadronic and electromagnetic particles with energies below the E_{\min}^{had} and E_{\min}^{em} are no longer treated by the cascade equations but traced again in the Monte Carlo scheme. The hadronic interactions at high energies are calculated with the QGSJET01 [18] model while the interactions at low energies with GHEISHA [24]. The electromagnetic interactions are treated by the EGS4 [25] code. The adopted kinetic energy cutoffs for all simulations were 50 MeV (0.3 MeV) for hadrons and muons (electrons and positrons). The forementioned energy thresholds were chosen in order to verify qualitatively the dependence and performance of the cascade results, trying to minimize the CPU time without the introduction of significant errors. All SENECA simulations were performed with 1.2.2. version.

III. RESULTS AND COMPARISONS

In this session we apply the SENECA simulation approach to generate gamma, iron nucleus and proton induced air showers at fixed primary energies and explore the longitudinal development. Although the simulation of showers at fixed energies is not a very realistic application we intend in the present work to compare quantitatively SENECA and CORSIKA results. One important reason for this comparison is to optimize the compromise between simulation time usage and accuracy in the description of fluctuations. In this particular case, such detailed study can be useful to many experiments which use the fluorescence technique.

In Fig. 1 we illustrate individual longitudinal profiles generated by SENECA (hybrid approach) code. Displayed cases correspond to median longitudinal profile produced for 1,000 gamma (dashed), iron nucleus (dot-dashed) and proton (solid) induced showers at 10^{19} eV, at zenith angle $\theta=45^\circ$ and free first interaction point. The shaded bands which follow each median line correspond to the upper limit of 68% of confidence level.

In order to make a simple comparison Fig. 2 illustrates the upper limit of 68% of confidence level for 1,000 SENECA profiles with 10 random showers simulated with CORSIKA. It is possible to see a very reasonable agreement among the several longitudinal profiles. In spite of that, we can verify that CORSIKA produces, apparently, more fluctuations related to individual proton and gamma air showers developments. All simulations performed by the CORSIKA code were obtained by using the thinning factor $t_f=10^{-6}$ and the same energy thresh-

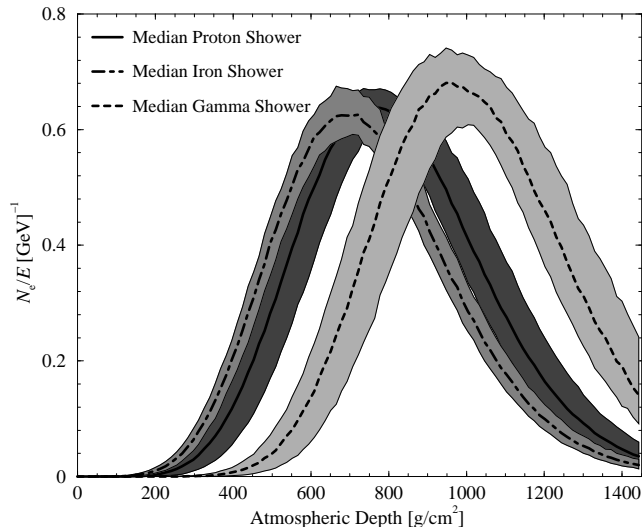


FIG. 1: Median longitudinal profile of electrons-positrons for 10 random gamma (dashed), iron nucleus (dot dashed) and proton (solid) induced showers at primary energy of 10^{19} eV, with zenith angle $\theta=45^\circ$, calculated by the SENECA scheme, by using the QGSJET01 hadronic interaction model. The shaded bands which follow each median line represent the upper limit of 68% of confidence level, for 1,000 simulated events.

old of SENECA simulations, 0.3 MeV (50 MeV) for photons and electrons (hadrons and muons).

To analyze more carefully the longitudinal profiles produced with the hybrid approach, we illustrate in Fig. 3 the number of electrons-positrons generated by 1,000 proton initiated showers at energy of 10^{19} eV, with zenith angle 45° , at arbitrary observation depths of (a) 200, (b) 400, (c) 600, (d) 800, (e) 1,000, and (f) 1,200 g/cm^2 . We compare the hybrid results (solid line) to the results obtained with CORSIKA (dashed line). The expected fluctuations due to very first proton interactions are reflected on panel (a) and (b), producing a difference of $\sim 4\%$ and $\sim 3\%$ between the distribution mean values. Panels (c) and (d) show discrepancies for the mean values of about 7% and 6%. In contrast to this, the discrepancies basically disappear at panels (e) and (f), both obtaining an agreement of about 99.5%. In all found discrepancies, SENECA produces more particles than CORSIKA. According to [16], some discrepancies are expected in the values produced for some shower quantities by the hybrid scheme and, apparently, are due to the combination of the used binning of discrete energy in the numerical solutions and the minimum energy threshold used for the electromagnetic cascade equations.

Such differences between the results of both codes at the first stages of the EAS development should not be crucial since depths around and after the shower maximum are the most important ones for all fluorescence experiments.

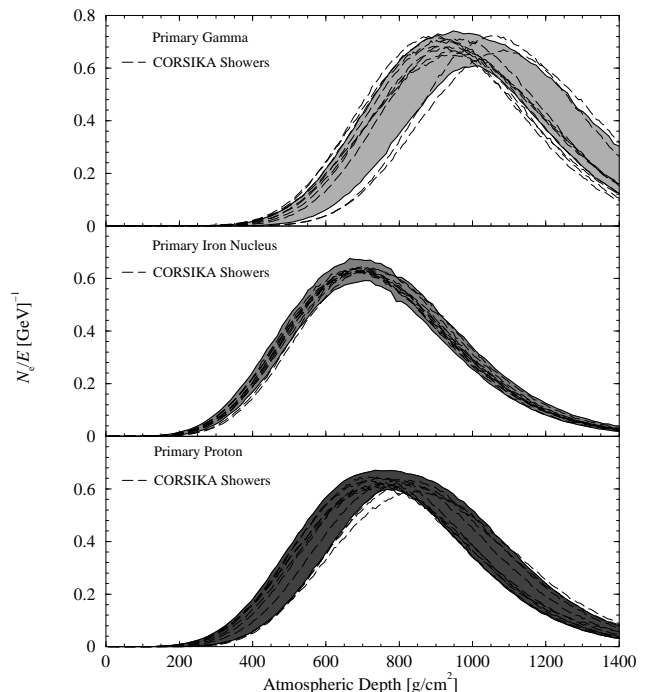


FIG. 2: Longitudinal profile of electrons-positrons for 10 random gamma, iron nucleus and proton initiated air showers at primary energy of 10^{19} eV, with incident zenith angle of 45° , calculated by the CORSIKA (long-dashed) code, with the QGSJET01 hadronic interaction model. The shaded curve in each panel represent the upper limit of 68% of confidence level for 1,000 events simulated with the SENECA code.

A. Analyses of influence of input parameters on shower quantities

In order to verify the dependence of the SENECA results, as suggested by the SENECA authors, on the combination of used energy binning and minimum energy threshold (E_{\min}^{em}) we have simulated air showers induced by gamma and proton primaries, with different initial conditions. Such primary particles have been chosen due to the different shower development in the atmosphere. The simulation development for gamma-induced showers deals mostly with the electromagnetic processes while the simulation development for proton (or any other hadron) showers deals with hadronic and electromagnetic processes. In other words, we are going to have different request of the cascade equation system for proton and gamma primary particles in the hybrid simulation.

1. S_{\max} Parameter

For the test with protons, 500 showers were generated of primary energy 10^{19} eV, with incident zenith angle of 45° , calculated with the hybrid method using 30, 40 and 50 bins (10 bins) in the numerical solutions of electromagnetic (hadronic) cascades, and different minimum en-

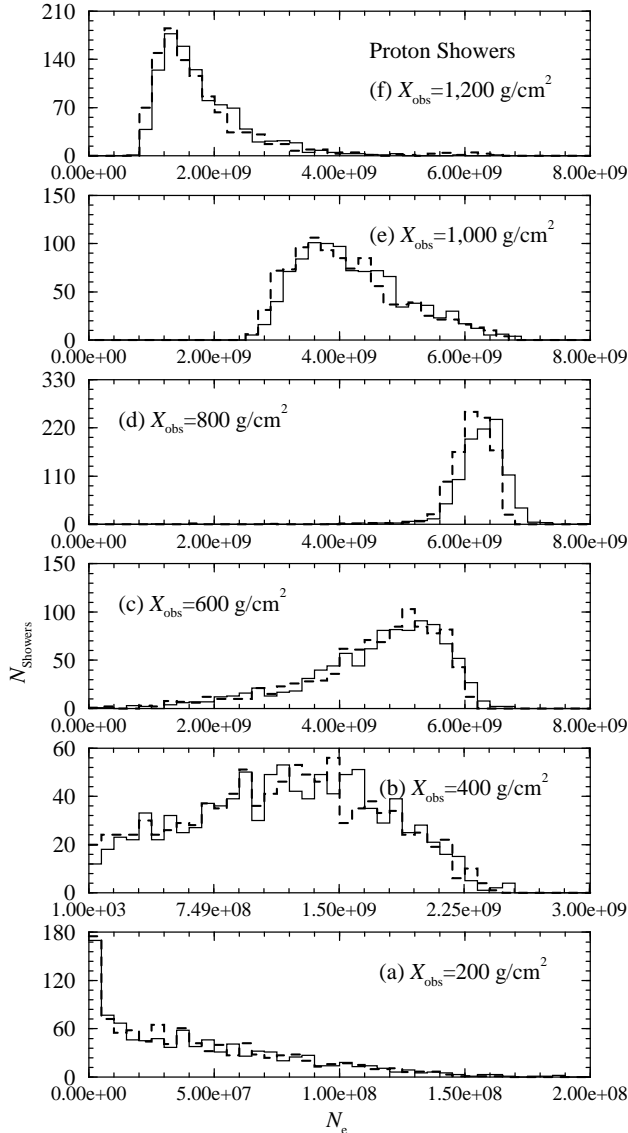


FIG. 3: Shower distribution in number of electrons at different slant depths. Results are shown for 1,000 showers, at 45° , generated by primary protons of energies 10^{19} eV calculated with the SENECA method (solid) and CORSIKA code (dashed), both using the QGSJET01 hadronic interaction model. Each panel represents a particular and arbitrary slant depth: (a) 200, (b) 400, (c) 600, (d) 800, (e) 1,000 and (f) 1,200, all in g/cm^2 .

ergy thresholds for the electromagnetic cascade equations $E_{\min}^{\text{em}} = 1, 10$ and 100 GeV. Following [16], we adopted $E_{\min}^{\text{had}} = 10^4$ GeV.

Fig. 4 shows the distribution of S_{\max} normalized by the primary energy in GeV, calculated with 500 primary protons by using 30 (panel a), 40 (panel b) and 50 (panel c) bins in the numerical solutions. The solid, dashed and dot-dashed lines correspond to $E_{\min}^{\text{em}} = 1, 10$ and 100 GeV, respectively, while the thick solid line refers to the distribution obtained with the CORSIKA code.

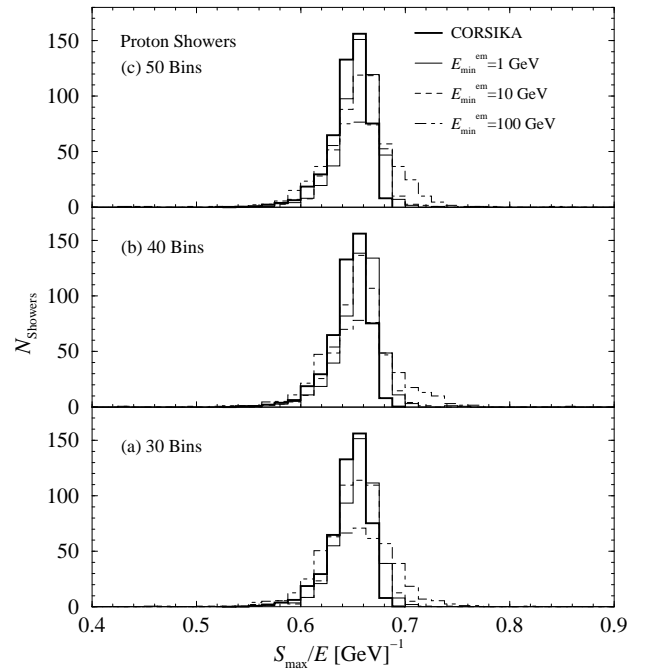


FIG. 4: Distribution of S_{\max} normalized by the primary energy in GeV. Results are shown for 500 proton showers of energy 10^{19} eV, with incident zenith angle of 45° , calculated with the hybrid scheme with different minimum energy thresholds and binnings of discrete energy, for the electromagnetic cascade equations. The thick solid line refers to the CORSIKA distribution. Both simulation codes generated the results by using the QGSJET01 hadronic interaction model. Panels (a), (b) and (c) refer to the parameter values of 30, 40 and 50 bins of discrete energy, respectively, in the numerical solutions of the hybrid simulations.

Although we have modified the inputs for the SENECA simulations, the average values of S_{\max}/E do not vary significantly and are in total agreement (99% on the average) with the average S_{\max}/E obtained with the CORSIKA shower generator. However, it is possible to verify in Fig. 4 that the S_{\max} distributions for the hybrid code are visibly wider for the minimum energy threshold values of 10 and 100 GeV, when compared to CORSIKA, showing a different behaviour for the S_{\max} fluctuations in both codes. Besides, such fluctuation description changes dramatically the characteristic asymmetrical shape of the S_{\max} distribution. The average (fluctuation) values of S_{\max}/E calculated with the hybrid scheme are presented in Table I and correspond to the distributions illustrated in Fig. 4. The average value obtained with the CORSIKA code is 0.646 while the width distribution is 2.06×10^{-2} .

Such S_{\max} fluctuation descriptions for the minimum electromagnetic energy threshold values of 10 and 100 GeV can clearly be seen as very strong dependence of shower quantities on initial parameters and are much larger when compared to the standard deviation value predicted by the CORSIKA code. One equally important aspect is that we have verified the dependence of

TABLE I: Average values of S_{\max} (standard deviation), normalized by the primary energy in GeV, obtained by hybrid simulations of 500 proton showers of primary energy $E = 10^{19}$ eV, with incident zenith angle of 45° . The predictions refer to the hybrid scheme by using different minimum electromagnetic energy threshold and distinct binnings of discrete energy. The average value obtained with the CORSIKA code is 0.646 while the sigma is 2.06×10^{-2} .

	30 Bins		40 Bins		50 Bins	
	S_{\max}/E	(σ)	S_{\max}/E	(σ)	S_{\max}/E	(σ)
$E_{\min}^{\text{em}}=1$ GeV	0.653	(2.08×10^{-2})	0.655	(2.75×10^{-2})	0.653	(2.85×10^{-2})
$E_{\min}^{\text{em}}=10$ GeV	0.651	(2.79×10^{-2})	0.653	(2.61×10^{-2})	0.654	(2.55×10^{-2})
$E_{\min}^{\text{em}}=100$ GeV	0.651	(4.27×10^{-2})	0.654	(4.05×10^{-2})	0.653	(4.09×10^{-2})

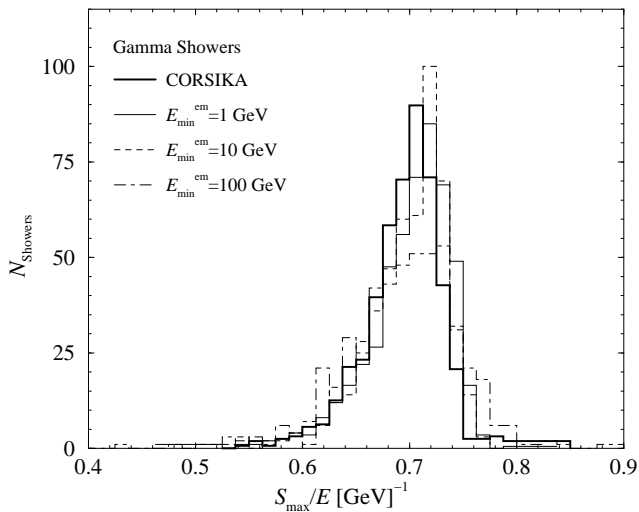


FIG. 5: Distribution of S_{\max} normalized by the primary energy in GeV. Results are shown for 500 primary gamma showers of energy 10^{19} eV, with zenith angle of 45° calculated with the SENECA and CORSIKA (thick solid line) schemes by using the QGSJET01 hadronic interaction model. The SENECA simulations were performed with different minimum energy thresholds for the electromagnetic cascade equations and the input value of 30 bins in the numerical solutions.

quantities on higher values of E_{\min}^{em} , while [16] expects the dependences on lower E_{\min}^{em} values.

The same unusual fluctuation description for S_{\max} can also be visualized in Fig. 5, which shows the S_{\max}/E distribution calculated with primary gammas by using 30 bins as input value in the numerical solutions. The thick solid line refers to the distribution obtained with the CORSIKA code. The average (sigma) values obtained from SENECA are $0.7 (4. \times 10^{-2})$, $0.698 (4.02 \times 10^{-2})$ and $0.694 (7.79 \times 10^{-2})$, for $E_{\min}^{\text{em}} = 1, 10$ and 100 GeV, respectively. The CORSIKA predicts the average S_{\max}/E distribution value of 0.694 and the width distribution of 4.74×10^{-2} .

Hence, these checks basically verify that, apparently,

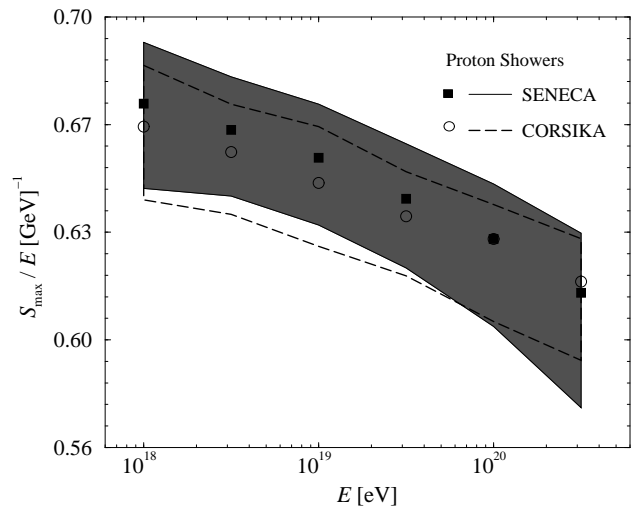


FIG. 6: Median values of the shower size at maximum air shower development (S_{\max}), normalized by the primary energy in GeV, related to proton-induced showers as a function of primary energy. The solid (long-dashed) line represents a band containing 68% of confidence level for 500 (100) events generated by the SENECA (CORSIKA) code, at $\theta = 45^\circ$, using the QGSJET01 hadronic interaction model. The full square (full circle) represents the median values of S_{\max} obtained with the SENECA (CORSIKA) code.

the minimum electromagnetic energy thresholds of 10 and 100 GeV may produce artificial fluctuations on S_{\max} . Moreover, such fluctuation description can introduce statistical errors on analyses of event-to-event and could be possible critics in practical applications of SENECA in fluorescence event reconstruction.

The increase in fluctuations with increasing E_{\min}^{em} , is difficult to understand since the larger the E_{\min}^{em} , the greater the weighted of the Monte Carlo portion of the hybrid scheme.

Fig. 6 shows the median shower size values, normalized by the primary energy in GeV, at the depth of shower maximum. Each band contains 68% of confidence

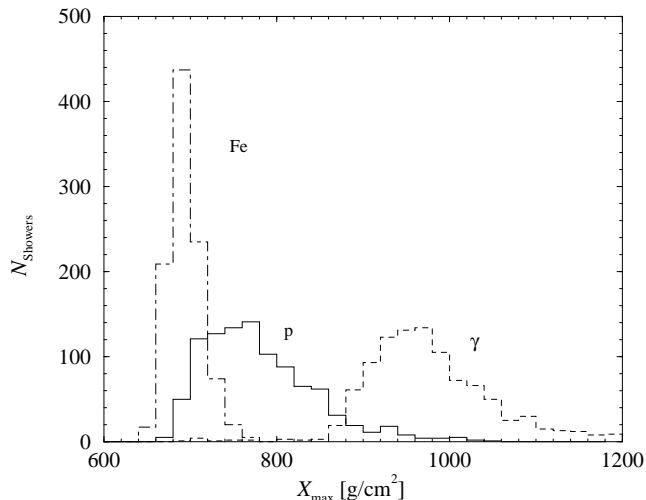


FIG. 7: Distribution of the depth of maximum air shower development shown for 1,000 proton, iron nucleus and gamma showers at a particular primary energy of 10^{19} eV, with incident zenith angle of 45° , calculated with the hybrid technique.

level and is related to proton initiated showers as a function of primary energy ($E > 10^{18}$ eV). The solid (dashed) line illustrates the predictions of the SENECA technique (CORSIKA), using the QGSJET01 model. We have used $E_{\min}^{\text{em}} = 1$ GeV and 30 bins of discrete energy as the input SENECA parameters.

The values predicted by both codes have a visible agreement ($> 99\%$). SENECA tends to produce systematically higher values of S_{\max} than CORSIKA, up to $10^{19.5}$ eV, and lower values for energies $> 10^{20}$ eV. Also, it seems that SENECA produces more fluctuations related to smaller shower sizes at energies around 10^{20} eV.

2. X_{\max} Parameter

As discussed in Sec. I, fluorescence detectors observe the longitudinal profile evolution by measuring the fluorescence light. The greatest advantage of this technique is that it allows the estimation of the number of charged particles as a function of depth in the atmosphere, from the measured data [26, 27, 28, 29], which makes possible, in turn, the estimation of the depth of maximum development of the shower, X_{\max} .

In principle, obtaining the values of X_{\max} and/or S_{\max} , by the fluorescence technique, and their respective fluctuations, by Monte Carlo, one should be able to reconstruct the shower energy and infer the identity of the primary cosmic ray [21, 28]. Fig.7 illustrates the potential of the X_{\max} distribution, generated with the hybrid scheme, to distinguish possible primary signatures, as calculated using SENECA.

We have also checked the behaviour of average X_{\max} values for gamma, iron nucleus and proton induced air shower.

Fig. 8 shows the average depth (bottom panel) and fluctuation (top panel) values of shower maximum (X_{\max}) for the energy range of 10^{18} - $10^{20.5}$ eV, with incident zenith angle of $\theta = 45^\circ$. All simulations performed in this plot were generated with the QGSJET01 hadronic interaction model. The long-dashed line represents 500 showers induced by gamma (diamond), iron nucleus (square) and proton (circle) primaries at each energy generated by SENECA. The CORSIKA predictions correspond to 100 simulated showers and are represented by solid lines and full symbols [30]. Only in Fig. 8 the CORSIKA results obtained for gamma showers were generated by using the PRESHOWER code. All other CORSIKA simulations in the present work were calculated without the PRESHOWER code.

The values predicted by both codes are in very good agreement, showing almost identical values for X_{\max} and fluctuations, for all primary particles. One interesting aspect to be mentioned is the strong influence of the geomagnetic field on depth of maximum development in gamma showers, generated by CORSIKA code [30] implemented with the PRESHOWER program [31], at energies above 10^{20} eV. The geomagnetic field decelerates the air gamma shower development, modifying the depth in

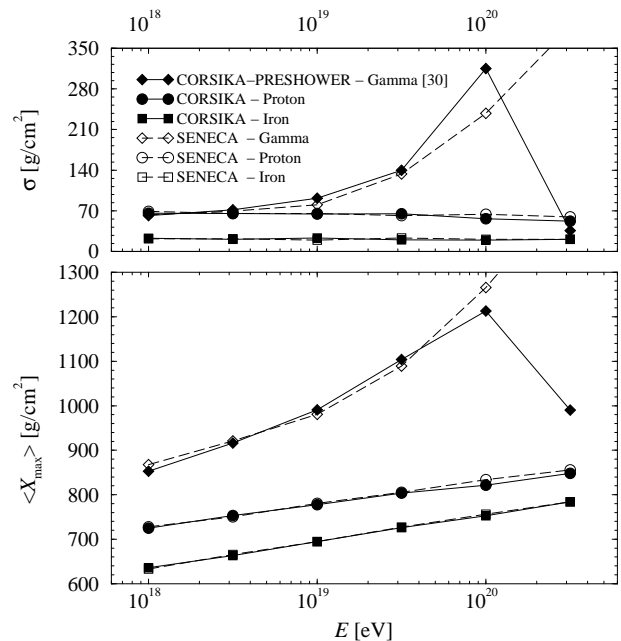


FIG. 8: Average depth (bottom panel) and sigma (top panel) values of maximum air shower development (X_{\max}) related to gamma, iron nucleus and proton induced showers as a function of extremely high primary shower energy, at $\theta = 45^\circ$, using the QGSJET01 hadronic interaction model. The long-dashed lines represent 500 events per energy induced by gamma (diamond), iron nucleus (square) and proton (circle) primaries generated by the SENECA. The CORSIKA predictions correspond to 100 simulated showers and are represented by solid lines and full symbols [30].

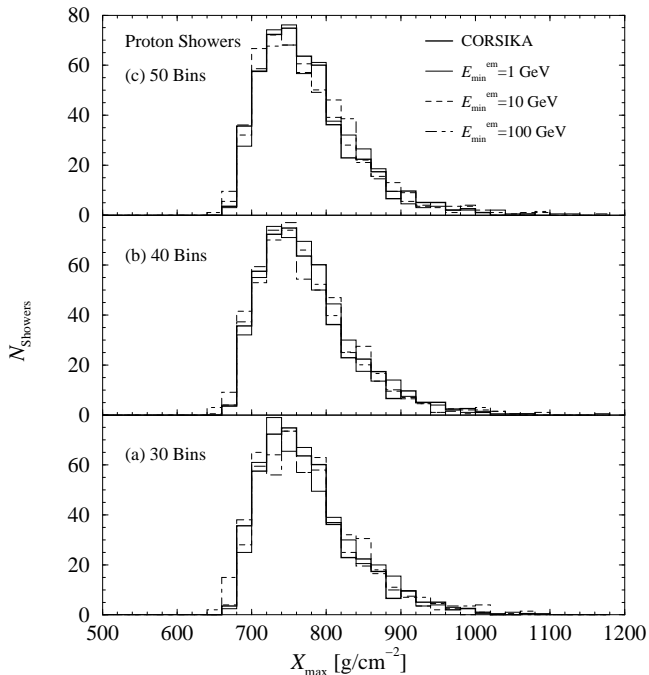


FIG. 9: Distribution of the depth of maximum air shower development. Results are shown for 500 proton showers of energy 10^{19} eV, with 45° , calculated with the SENECA by using different minimum energy thresholds and binnings of discrete energy, for the electromagnetic cascade equations. The thick solid line refers to the CORSIKA distribution. Both simulation codes generated the results by using the QGSJET01 hadronic interaction model. Panels (a), (b) and (c) refer to the parameter values of 30, 40 and 50 bins of discrete energy, respectively, in the numerical solutions of the hybrid simulations.

which occurs the maximum development. The average (fluctuation) value of X_{\max} decreases from 1,213 (314) g/cm^2 at 10^{20} eV to 990 (35) g/cm^2 at $10^{20.5}$ eV. Although we have considered the geomagnetic field in our simulations, it seems that SENECA do not consider the interaction of ultra high energy photons with the Earth's geomagnetic field before entering the Earth's atmosphere. Such effect absence produces the discrepancy seen in gamma curves at energies above and around 10^{20} eV. References [32, 33] discuss very high energy gamma showers.

Fig. 9 confirms the strength of the agreement by showing the distribution of X_{\max} values, produced by 500 proton showers, for the particular primary energy 10^{19} eV, with incident zenith angle of 45° , calculated with SENECA and CORSIKA (thick solid line) codes and QGSJET01 hadronic interaction model. We used the same input parameters for SENECA as in Fig. 4. The mean (fluctuation) X_{\max} values calculated with the hybrid scheme are presented in Table II. These values are in total agreement with CORSIKA values, $\langle X_{\max} \rangle = 774 \text{ g}/\text{cm}^2$ ($\sigma = 65 \text{ g}/\text{cm}^2$), and show, apparently, that the influence of minimum energy threshold and binning of discrete energy on X_{\max} values is negligible in

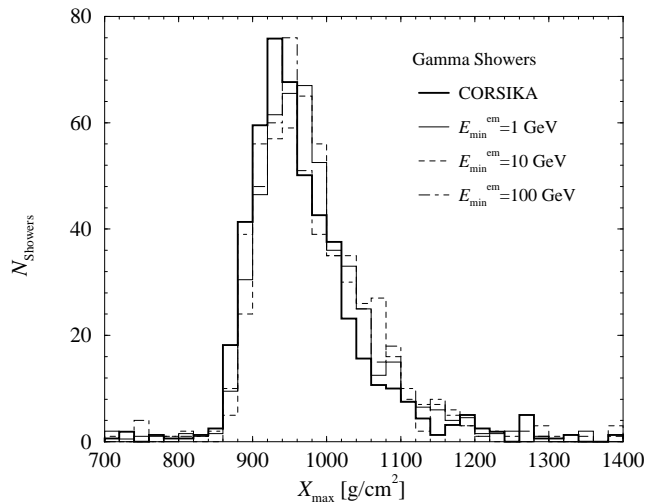


FIG. 10: Distribution of the depth of maximum air shower development. Results are shown for 500 gamma showers of energy 10^{19} eV, with incident zenith angle of 45° , calculated by the hybrid scheme with different minimum energy thresholds for the electromagnetic cascade equations. The thick solid line refers to the CORSIKA distribution. The obtained values refer to 30 bins of discrete energy in the numerical solutions of the hybrid simulations.

hadron initiated showers.

We have made the same X_{\max} verification for gamma showers in Fig. 10 and we verify that CORSIKA and SENECA distributions are in good agreement. SENECA predicts the average (fluctuation) X_{\max} distribution values of 981 g/cm^2 (81 g/cm^2), 989 g/cm^2 (85 g/cm^2) and 985 g/cm^2 (101 g/cm^2), for minimum electromagnetic energy thresholds of 1, 10 and 100 GeV, respectively. CORSIKA code, without PRESHOWER, produces the average and width distribution values of 976 g/cm^2 and 97 g/cm^2 , respectively. Due to the extreme fluctuations in shower development induced by primary gammas, which affect directly the position of shower maximum development, the average and fluctuation results obtained by SENECA seem to be reasonable, in spite of the fact that again the fluctuation values increase with the electromagnetic minimum energy thresholds of 10 and 100 GeV, over those of CORSIKA.

3. S_{\max} - X_{\max} Correlation

We also analyzed the correlation between S_{\max} and X_{\max} , which are important longitudinal shower quantities on event reconstruction. We compared SENECA results with CORSIKA predictions for gamma and proton induced air shower.

Fig. 11 shows the correlation between these parameters for both simulation schemes. We simulated 500 gamma showers for each code, of energy 10^{19} eV, incident zenith angle $\theta = 45^\circ$ and free first interaction point. Hybrid re-

TABLE II: Average (standard deviation) values of X_{\max} , all in g/cm^2 , obtained by hybrid simulations of 500 proton showers of primary energy $E = 10^{19}$ eV, with incident zenith angle of 45° . The predictions refer to the hybrid scheme by using different minimum electromagnetic energy threshold and distinct binnings of discrete energy. The average value obtained with the CORSIKA code is $774 \text{ g}/\text{cm}^2$ while the sigma is $65 \text{ g}/\text{cm}^2$.

	30 Bins	40 Bins	50 Bins
	X_{\max} (σ)	X_{\max} (σ)	X_{\max} (σ)
$E_{\min}^{\text{em}}=1 \text{ GeV}$	778 (65)	775 (63)	776 (64)
$E_{\min}^{\text{em}}=10 \text{ GeV}$	775 (62)	772 (61)	774 (65)
$E_{\min}^{\text{em}}=100 \text{ GeV}$	774 (69)	771 (66)	777 (70)

sults are shown for minimum energy thresholds $E_{\min}^{\text{em}} = 1$ (crosses) and 100 GeV (squares), and 30 bins of discrete energy in the numerical solutions. The full circles denote the corresponding values for CORSIKA. It is possible to verify the existence of large fluctuations in gamma air showers at this particular primary energy.

The small box in the figure encloses, approximately, the highest density of correlation points for both codes: 61% and 59% of the total number of events simulated by SENECA, for $E_{\min}^{\text{em}} = 1$ and 100 GeV, respectively, and 64% of the total showers generated with CORSIKA.

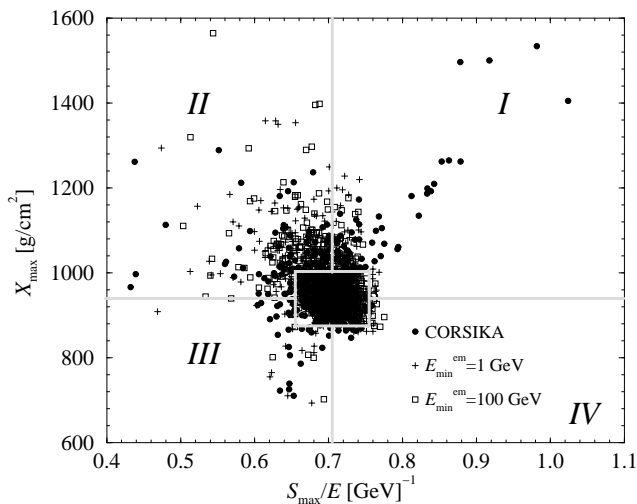


FIG. 11: The correlation between X_{\max} and S_{\max}/E for gamma induced showers at primary energy 10^{19} eV, at zenith angle $\theta = 45^\circ$, obtained with SENECA and CORSIKA codes. The full circles represent 500 showers simulated with CORSIKA, while square and cross symbols illustrate 500 events generated with the hybrid method, by using minimum electromagnetic energy thresholds $E_{\min}^{\text{em}} = 1$ and 100 GeV, respectively.

The number of gamma showers predicted by SENECA and CORSIKA vary considerably from one quadrant to another in Fig. 11, indicating qualitative and quantitative differences in the character of the fluctuations in both

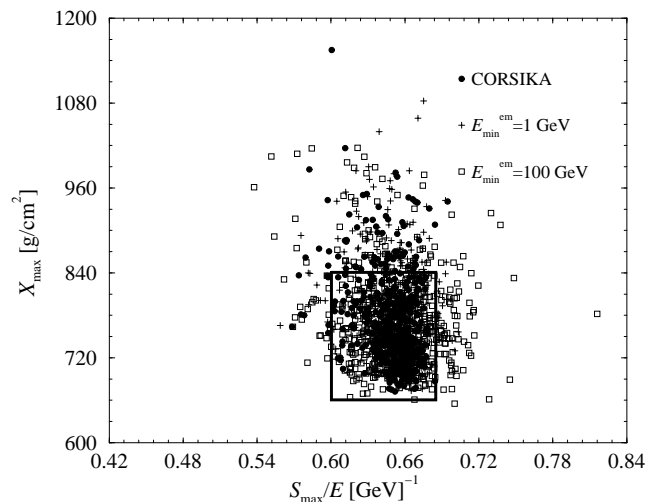


FIG. 12: The correlation between X_{\max} and S_{\max}/E for proton induced showers at primary energy 10^{19} eV, at zenith angle $\theta = 45^\circ$, obtained with SENECA and CORSIKA codes. The full circles represent 500 showers simulated with CORSIKA, while square and cross symbols correspond to 500 showers generated with the hybrid method, by using minimum electromagnetic energy thresholds $E_{\min}^{\text{em}} = 1$ and 100 GeV, respectively.

codes.

The fractions of events inside regions I, II, III and IV (see the figure) are, respectively, 10% (10%), 24% (27%), 3% (2%) and 2% (2%), for the minimum energy threshold of 1 (100) GeV. In the same regions, the corresponding CORSIKA fractions are 11%, 17%, 6% and 2%.

Notoriously, CORSIKA shows in region I a particular structure related to maximum depth development ($X_{\max} > 940 \text{ g}/\text{cm}^2$) of particularly large showers ($S_{\max}/E > 0.705$). Such structure is absent in SENECA.

On the other hand, the hybrid scheme predicts a significantly number of ordinary and small showers in region II (118 and 137 showers for $E_{\min}^{\text{em}} = 1$ and 100 GeV, respectively), which achieve higher values for the depth of

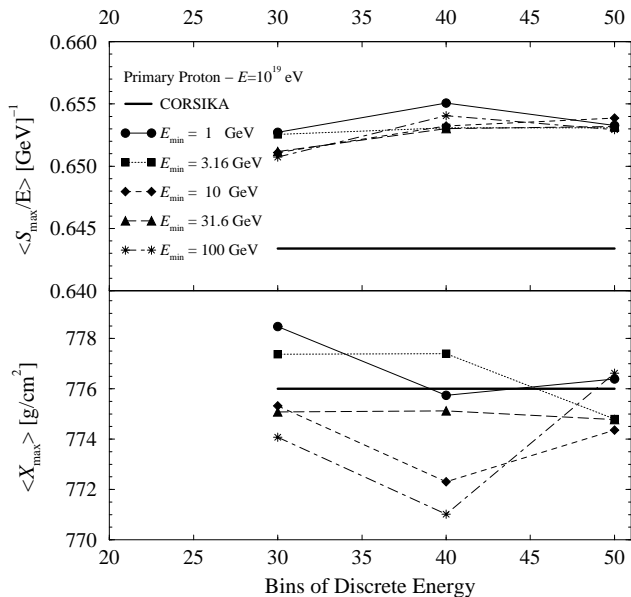


FIG. 13: Average values of X_{\max} and S_{\max}/E for 1,000 proton induced showers at primary energy 10^{19} eV, at zenith angle $\theta = 45^\circ$, obtained with SENECA and CORSIKA (thick solid line) codes (see the text).

maximum development, a behavior that is not as strong in CORSIKA (84 showers).

The same kind of comparison is presented in Fig. 12 for proton showers. The same input parameters as in the previous figure were used to simulate the three sets of 500 proton showers each displayed in Fig. 11.

It is apparent from the figure that the hybrid approach generates a more scattered distribution of showers, with wider tails, than CORSIKA does.

This is confirmed by counting the number of events inside the small box shown in the figure. SENECA expectation amounts to 80% (69%) of the proton showers falling inside the box for $E_{\min}^{\text{em}} = 1$ and 100 GeV, while CORSIKA expectation is 85%.

We can verify in SENECA predictions that the input parameter $E_{\min}^{\text{em}} = 100$ GeV produces larger fluctuations related to proton shower size ($\sigma_{S_{\max}/E}$), describing a sort of symmetrical distribution of events outside the box. The standard deviation of proton shower size, obtained for this particular input parameter in SENECA, is 3.62×10^{-2} while the corresponding value for CORSIKA is 1.89×10^{-2} . Such symmetrical statement is confirmed in Fig. 4.

Figs. 13 and 14 illustrate the dependence of the average values, and their fluctuation, of X_{\max} and S_{\max} on input parameters of electromagnetic cascade equations solved in SENECA scheme. We have generated 1,000 proton showers, at primary energy 10^{19} eV and zenith angle $\theta = 45^\circ$, using 30, 40 and 50 bins of possible discrete energy for each minimum energy threshold; total of 15,000 simulated events. As it has been

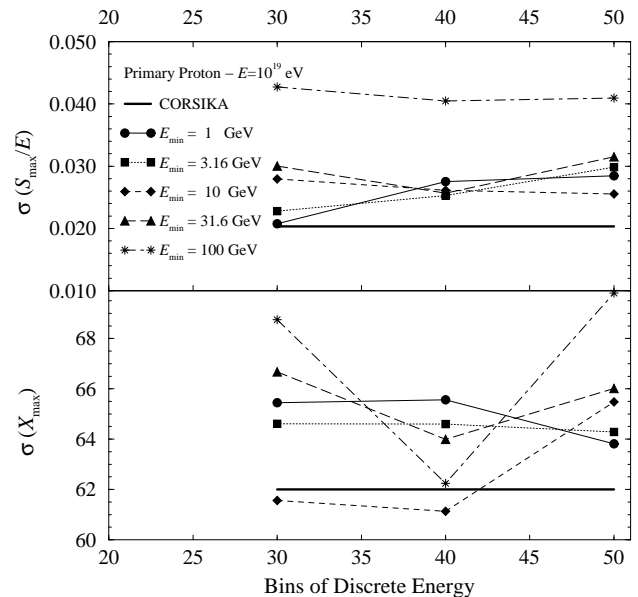


FIG. 14: Fluctuation of the position of shower maximum and maximum shower size, for 1,000 proton induced showers at primary energy 10^{19} eV, at zenith angle $\theta = 45^\circ$, obtained with SENECA and CORSIKA (thick solid line) codes (see the text).

noted in top panel of Fig. 13, the average values produced by SENECA are in perfect agreement (>99% for both quantities) with the corresponding results obtained from CORSIKA (thick solid line).

However, Fig. 14 shows that the fluctuations related to S_{\max} (top panel) have large discrepancies for a minimum electromagnetic energy threshold of 100 GeV. In this case, there is more than a factor of 2 between SENECA and CORSIKA expected fluctuation levels ($\sigma \sim 4.15 \times 10^{-2}$, averaged over number of bins, vs. $\sigma \sim 2.034 \times 10^{-2}$ in the case of CORSIKA).

On average, the discrepancies in σ between SENECA and CORSIKA decrease systematically at progressively lower values of E_{\min}^{em} .

Even if fluctuations in X_{\max} can be up to 8% larger in SENECA than in CORSIKA (for $E_{\min}^{\text{em}} = 100$ GeV) this discrepancy is of small practical relevance when translated into units of depth (i.e., in g/cm^2).

4. N_μ - Number of muons

To ensure the consistency of other longitudinal shower components in SENECA, we have also compared the number of muons produced by both SENECA and CORSIKA codes.

Fig. 15 shows the muon component for 1,000 proton initiated showers at energy of 10^{19} eV and incident zenith angle of 45° , at observation depths of (a) 200, (b) 400, (c) 600, (d) 800, (e) 1,000, and (f) 1,200 g/cm^2 . As we

can seen, both distribution agree very well. The average number of muons are very similar (99% of coincidence) when related to the first stages of shower development, panels (a), (b) and (c). At the same time, discrepancies become greater with depths closer to the sea level, but are on average less than $\sim 3\%$ (2% at 800 g/cm^2 , 3.6% at $1,000 \text{ g/cm}^2$ and 3.3% at $1,200 \text{ g/cm}^2$). Such small discrepancies can be considered negligible, because they are undetectable to any experiment which measures the correlated number of particles. Furthermore, the fluctuations (width distribution) corresponding to each panel agree well with those predicted in CORSIKA code. Consequently, the muon distributions seem to be well described in the hybrid scheme when compared to the CORSIKA ones.

5. Processing time consumption

As a final comparison, we show in Table III the impressive numbers related to the rate of time-consumption ($T_{\text{CORS}}/T_{\text{SEN}}$) between the CORSIKA and SENECA codes. All simulations generated with CORSIKA were obtained by using the thinning factor $t_f=10^{-6}$.

In order to compare the time-consuming of the hybrid method, by using the thinning procedure in the Monte Carlo calculation, we have generated air showers with thinning level of 10^{-6} for the Monte Carlo scheme.

In Table III, Rate-1 refers to the hybrid simulations without the thinning procedure while Rate-2 considers the SENECA simulations by using the thinning procedure with thinning level of 10^{-6} in the Monte Carlo scheme.

IV. DISCUSSION AND CONCLUSIONS

In the present work we analyzed the practical potential of SENECA, a very fast hybrid tri-dimensional code, for the simulation of the longitudinal development of extensive air showers at high energies. We take as reference the well known and extensively tested CORSIKA code, which is based on a much slower, but highly reliable, full Monte Carlo simulation. The QGSJET01 hadronic interaction model is used throughout the paper for both codes.

Although a careful analysis of many shower quantities discussed here is strongly model dependent, we are confident that the present study is able to show the potential and limitations of SENECA, in its present version, for a practical application to the analysis of fluorescence data on ultra-high energy cosmic rays.

The consistency of the SENECA scheme was tested and it proved to be very stable for energies above 10^{18} eV. The results obtained by both codes agree well with negligible discrepancies for most quantities analyzed.

Apparently, minimum electromagnetic energy threshold values of 10 and 100 GeV may produce artificial

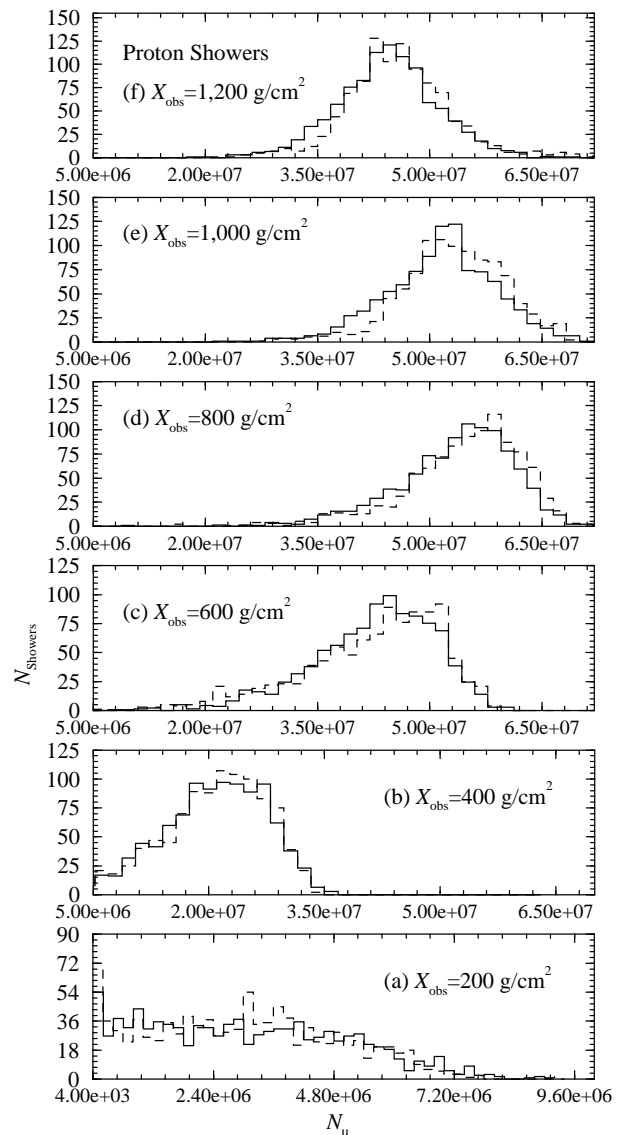


FIG. 15: Shower distribution in number of muons at different slant depths. Results are shown for 1,000 showers, at 45° , generated by primary protons of energies 10^{19} eV calculated with the SENECA method (solid) and CORSIKA code (dashed), both using the QGSJET01 hadronic interaction model. Each panel represents a particular and arbitrary slant depth: (a) 200, (b) 400, (c) 600, (d) 800, (e) 1,000 and (f) 1,200, all in g/cm^2 .

fluctuations on S_{max} shower quantity. These could be responsible for the introduction of systematic errors on the analysis of isolated events and should be taken into account when applying SENECA to fluorescence reconstruction.

In any case, the undisputable bounty of SENECA is velocity. The rates of processing time-consumption between CORSIKA and SENECA are, to say the least, impressive over the wide range of primary shower energy tested here.

TABLE III: Rate of time-consuming between CORSIKA and SENECA codes, i.e., $\text{Rate} = T_{\text{CORS}}/T_{\text{SEN}}$. Rate-1 refers to the hybrid scheme with the traditional Monte Carlo method, while Rate-2 considers the hybrid scheme using the thinning level of 10^{-6} in the Monte Carlo. All CPU times used for the calculation of the rate refer to a 2.1 GHz AMD Athlon processor.

$\log_{10} E_0$ [eV]	Rate-1	Rate-2
17.0	3	13
17.5	3	13
18.0	4	15
18.5	5	16
19.0	7	20
19.5	11	28
20.0	20	46
20.5	35	74

Finally, as a word of caution, special attention must be paid to the selection of the several input parameters of SENECA in practical applications, since they may affect the results in a non-trivial and somehow unpredictable way.

Acknowledgments The authors acknowledge Hans-Joachim Drescher and Glennys Farrar for making SENECA code available to the cosmic ray academic com-

munity. We are indebted to Dieter Heck for providing us with the values of X_{max} for CORSIKA. J.A.Ortiz is supported by CNPq/Brazil, G.M.T. by FAPESP and CNPq and L.V. Souza by FAPESP. Most of the simulations presented here were carried on a Cluster Linux TDI (32 Dual Xeon 2.8 GHz, 2GBytes RAM nodes), supported by Laboratório de Computação Científica Avançada at Universidade de São Paulo.

-
- [1] J. Linsley, L. Scarsi, and B. Rossi, Phys. Rev. Lett. **6**, 458 (1961).
 - [2] J. Linsley, Phys. Rev. Lett. **34**, 146 (1963).
 - [3] M. A. Lawrence, R. J. O. Reid, and A. A. Watson, J. Phys. G **17**, 733 (1991).
 - [4] B. Afanasiev *et al.*, in *Proceedings of the the International Symposium on Extremely High Energy Cosmic Rays: Astrophysics and Future Observatories*, edited by M. Nagano (Institute for Cosmic Ray Research, University of Tokyo, Tokyo, Japan, 1996), p. 32.
 - [5] R. M. Baltrusaitis *et al.*, Nucl. Instrum. Meth. Phys. Res. A **264**, 87 (1988).
 - [6] D. J. Bird *et al.*, Astrophys. J. **441**, 144 (1995).
 - [7] HiRes Collaboration, T. Abu-Zayyad *et al.*, Nucl. Instrum. Meth. Phys. Res. A **450**, 253 (2000).
 - [8] N. Chiba *et al.*, Nucl. Instrum. Methods Phys. Res. A **311**, 338 (1992).
 - [9] N. Hayashida *et al.*, Phys. Rev. Lett. **73**, 3491 (1994).
 - [10] Pierre Auger Collaboration, J. Blumer *et al.*, J. Phys. G: Nucl. Part. Phys. **29**, 867 (2003).
 - [11] Pierre Auger Collaboration, J. Abraham *et al.*, Nucl. Instrum. Meth. Phys. Res. A **523**, 50 (2004).
 - [12] R. Engel and H. Klages, C. R. Physique **5**, 505 (2004).
 - [13] G. Bossard *et al.*, Phys. Rev. D **63**, 054030 (2001).
 - [14] T. Pierog *et al.*, astro-ph/0411260.
 - [15] J. Alvarez-Muñiz *et al.*, Phys. Rev. D **66**, 033011 (2002).
 - [16] H. J. Drescher and G. R. Farrar, Phys. Rev. D **67**, 116001 (2003).
 - [17] N. N. Kalmykov and S. S. Ostapchenko, Phys. At. Nucl. **56**, 346 (1993).
 - [18] N. N. Kalmykov, S. S. Ostapchenko, and A. I. Pavlov, Nucl. Phys. B (Proc. Suppl.) **52B**, 17 (1997).
 - [19] D. Heck, J. Knapp, J. N. Capdevielle, G. Schatz, and T. Thouw, Report FZKA 6019 (1998).
 - [20] H. J. Drescher, astro-ph/0411144.
 - [21] J. Cronin *et al.*, The Pierre Auger Project design report 2nd ed., available at Auger website www.auger.org (1995).
 - [22] HiRes Collaboration, T. Abu-Zayyad *et al.* astro-ph/0208301.
 - [23] O. Catalano, Nuovo Cim. **24C**, 445 (2001).
 - [24] H. Fesefeldt, PITHA 85/02, RWTH Aachen (1985).
 - [25] W. Nelson *et al.*, SLAC-265, Stanford Linear Accelerator Center (1985).
 - [26] C. Song *et al.*, Astropart. Phys. **14**, 7 (2000).
 - [27] R. M. Baltrusaitis *et al.*, Nucl. Instrum. Meth. Phys. Res. A **240**, 410 (1985).
 - [28] J. Alvarez-Muñiz *et al.*, Phys. Rev. D **69**, 103003 (2004).
 - [29] H. M. J. Barbosa, F. Catalani, J. A. Chinellato, and C. Dobrigkeit, astro-ph/0310234.
 - [30] D. Heck, (private communication).
 - [31] P. Homola *et al.*, astro-ph/0311442.
 - [32] P. Homola *et al.*, Acta Phys. Polon. B **35**, 1893 (2004).
 - [33] M. Risse *et al.*, Astropart. Phys. **21**, 479 (2004).